A non-resonant rotational electromagnetic energy harvester for low-frequency and irregular human motion

Huicong Liu, Cheng Hou, Jiahong Lin, Yunfei Li, Qiongfeng Shi, Tao Chen, Lining Sun, and Chengkuo Lee

Citation: Appl. Phys. Lett. **113**, 203901 (2018); doi: 10.1063/1.5053945
View online: https://doi.org/10.1063/1.5053945
View Table of Contents: http://aip.scitation.org/toc/apl/113/20
Published by the American Institute of Physics

APPLIED PHYSICS LETTERS **113**, 203901 (2018)

A non-resonant rotational electromagnetic energy harvester for low-frequency and irregular human motion

Huicong Liu,[1] Cheng Hou,[1] Jiahong Lin,[1] Yunfei Li,[1] Qiongfeng Shi,[2,3,4,5] Tao Chen,[1,2,3,4,5,a)] Lining Sun,[1] and Chengkuo Lee[2,3,4,5,a)]

[1]*School of Mechanical and Electric Engineering, Jiangsu Provincial Key Laboratory of Advanced Robotics, Soochow University, Suzhou 215123, China*
[2]*Department of Electrical and Computer Engineering, National University of Singapore, 4 Engineering Drive 3, Singapore 117576, Singapore*
[3]*Center for Intelligent Sensors and MEMS, National University of Singapore, E6 #05-11F, 5 Engineering Drive 1, Singapore 117608, Singapore*
[4]*Hybrid-Integrated Flexible (Stretchable) Electronic Systems Program, National University of Singapore, E6 #05-4, 5 Engineering Drive 1, Singapore 117608, Singapore*
[5]*National University of Singapore Suzhou Research Institute (NUSRI), Suzhou Industrial Park, Suzhou 215123, China*

(Received 28 August 2018; accepted 29 October 2018; published online 12 November 2018)

There is an abundance of low-frequency and irregular human motion energy that can be harvested. In this work, a non-resonant rotational electromagnetic energy harvester (REH) for scavenging low-frequency (<10 Hz) and irregular human motion is presented. The energy harvester simply introduces a cylindrical stator and a disk-shaped rotor forming a movement of a higher pair. Without any complicated transmission mechanism, the rotor can easily rotate around the stator by magnetic attractive force. Driven by a broadband frequency vibration, the magnetic rotor is coupled with surrounding wound coils to operate electromagnetic energy harvesting. Theoretical and experimental investigations of the REH are studied, and numerical simulations show good agreement with the experimental results. The treadmill tests at various motion speeds are performed to demonstrate the advantage of the REH in harvesting energy from irregular human motion. At a driving frequency of 8 Hz, the electromagnetic coils can provide the maximum power of 10.4 mW at a load resistance of 100 Ω. The REH exhibits outstanding output performance and has potential applications for powering intelligent wearable or portable electronic devices. *Published by AIP Publishing*. https://doi.org/10.1063/1.5053945

In recent years, harvesting kinetic energy from human motion has been extensively studied, as it can potentially achieve energy autonomy for wearable electronics and portable devices.[1,2] There are three major mechanisms for vibration energy harvesting, which are piezoelectric,[5–8] electromagnetic,[11–14] and triboelectric.[3,4] Various piezoelectric and electromagnetic energy harvesters have been explored due to their advantages of simple configuration and high output performance.[6,7] However, the main disadvantage of such linear resonant harvesters is that the output power drops dramatically under off-resonance conditions. Realizing a multiple resonant mode of a harvester is an efficient way to deal with the narrow bandwidth issue.[11–13] Meanwhile, this issue has inspired intensive investigations of nonlinear mechanisms to broaden the operation bandwidth and improve the energy harvesting efficiency.[9,14–21] A nonlinear electromagnetic energy harvester from hand shaking was presented in our previous work.[9,10] The nonlinear magnetic-spring configuration was employed for generating sufficient power from hand shaking of irregular and low-frequency vibrations. Pit *et al.*[16] introduced an inertial energy harvester for human body applications combining the frequency up-conversion principle, in the form of piezoelectric beam plucking through magnetic coupling with a rotating proof mass. Fan *et al.*[17] developed a nonlinear piezoelectric energy harvester via introducing the magnetic coupling between a ferromagnetic ball and four piezoelectric cantilever beams. The numerical and experimental performances of bi-stable[18] and tri-stable[19] nonlinear harvesters with different potential well functions were investigated under harmonic excitations by Cao *et al.* In addition, Zhou *et al.*[20] and Wang *et al.*[21] proposed similar nonlinear monostable and bi-stable energy harvesters to broaden the bandwidth from low-level ambient vibrations, respectively.

Considering the characteristics of human motion such as walking, running, and arm shaking, the random and irregular vibrations are always at ultra-low frequency (<10 Hz). The nonlinear energy harvesters reported above were operated at relatively high frequencies and cannot efficiently harvest human motion energy. Moreover, the reported energy harvesters work in a single direction of vibration, and the amount of power is limited due to the irregular magnitude and direction of vibrations. On the contrary, unlimited rotary motion could be used to eliminate the restriction of traditional linear and nonlinear harvesters. Spreemann *et al.*[22] presented a non-resonant rotational vibration-to-electrical power generator which can scavenge for a wide frequency spectrum. Pan *et al.*[23] and Yang *et al.*[24] successively proposed an in-plane rotary electromagnetic micro-generator. Then, an energy-harvesting system integrating a hula-hoop motion transformer was proposed by Lu *et al.*,[25,26] which can scavenge energy from machinery or human body. When

[a)]Authors to whom correspondence should be addressed: chent@suda.edu.cn and elelc@nus.edu.sg

the external excitation frequency was 8 Hz, the maximum power of the system can be about 5 mW. In a recent article, Halim *et al.*[27] designed an electromagnetic rotational energy harvesting device using an improved eccentric rotor structure to harvest kinetic energy from a pseudo-walking signal. The prototype with optimal spring stiffness generated a maximum power of 61.3 μW at the rotational amplitudes of $\pm 25°$ and the frequency of 1 Hz. Therefore, such a rotational electromagnetic energy harvester can easily scavenge energy from walking and running in daily life.

It is a great challenge to work out a resonant system working at a high g or amplitude but a low frequency (<10 Hz) shaking condition. In this work, we developed a non-resonant rotational electromagnetic energy harvester with a simple configuration that can meet these criteria. The energy harvester simply introduces a cylindrical stator and a disk-shaped rotor forming a movement of higher pair. Under the excitation such as linear reciprocating motion, rotary motion, and swing motion in different directions, the rotor can easily rotate around the stator by the magnetic attractive force. Theoretical simulations and experimental tests show that the proposed rotational electromagnetic energy harvester (REH) can not only harvest energy from the ultra-low frequency (0–10 Hz) of human motion but also be sensitive to vibration excitation along multiple directions. Different excitations including linear reciprocating motion, rotary motion, and swing motion were evaluated. In addition, the proposed REH was attached on one tester's wrist and ankle to harvest random walking and running motion energy on the treadmill at ultra-low frequencies.

A schematic diagram of the proposed REH is shown in Fig. 1(a), which consists of a magnetic stator, a magnetic rotor, and four wound coils embedded in a bottom casing with a dimension of Φ65 mm in diameter and 18 mm in height. A cover is fixed on the top of the casing by bolt. Both the stator and rotor are made of NdFeB magnets. The cylindrical stator magnet of Φ10 mm × 5 mm is fixed in the center of the casing, and the disk-shaped rotor magnet of Φ25 mm × 3 mm is attached on the circle edge of the stator by the magnetic attractive force F_M. Without assembling any shaft or bearing structure, the magnetic stator and rotor of theoretical line contact formed a higher pair of movement. A small displacement of the external excitation will lead to the attraction of the stator to the rotor, thus making the rotor rotate around the stator. Therefore, the magnetic rotor can be easily driven to do clockwise and anticlockwise rotation around the center stator by external excitation force, avoiding unnecessary surface friction. An excitation from any direction is able to trigger the rotor rotation around the stator to achieve energy harvesting. Meanwhile, due to the magnetic attraction force, the rotor could not leave the stator by the influence of centrifugal force within a certain range of angular velocity. The four wound coils are arranged in a circular pattern around the center stator, and each has a dimension of Φ25 mm × 4 mm. The coils are connected in series. Figure 1(b) shows the magnetic field distribution of the stator and rotor. The rotational motion of the rotor magnet will induce a magnetic line cutting across each wound coil, and electrical voltage will be induced in the electromagnetic coil accordingly. Two typical application scenarios for the REH are shown in Fig. 1(c). For human walking and running, the rotor magnet of the REH attached on the wrist and ankle does clockwise and anticlockwise rotation around the center stator magnet. Figure 1(d) shows the physical model of the REH when the rotor magnet rotates under external force F applied in the y-direction. M, m, C_m, C_e, R, r, θ, and f denote the mass of the housing, the rotor magnet mass, the rotational damping force due to the friction between the stator and the rotor magnet, the electric-magnetic resistance force due to the rotating between the rotor magnet and coils, the radius of rotor magnet, the radius of the stator magnet, the angle at which the rotor rotates, and the inertia force, respectively. In the simulation, the REH is confined to be excited along the y-direction and parallel to the ground. No gravitational force affects its motion. On the basis of the dynamic characteristics of the model, the motion of the stator magnet is defined as $x_m = (R + r)\sin\theta$ and $y_m = y + (R + r)\cos\theta$, where x_m and y_m denote the absolute displacements of the rotor magnet in the x- and y-directions, respectively. y denotes the reciprocating motion of the main mass. By differentiating x_m and y_m with respect to time, the velocity of rotor magnet can be obtained as $\dot{x}_m = (R + r)\dot{\theta}\cos\theta$ and $\dot{y}_m = \dot{y} - (R + r)\dot{\theta}\sin\theta$. Then, the kinetic energy T can be expressed as

$$T = \frac{1}{2}M\dot{y}^2 + \frac{1}{2}m\left(\dot{y}^2 + 2(R + r)\dot{y}\dot{\theta}\sin\theta + (R + r)^2\dot{\theta}^2\right) + \frac{1}{2}I\dot{\theta}^2, \quad (1)$$

where I is the mass moment of inertia of the rotor magnet. With the kinetic energy, potential energy, and generalized forces, the equations describing the motion of the system can be derived by using Lagrange's equations. Thus, the equations governing the motion of the rotor magnet are written as

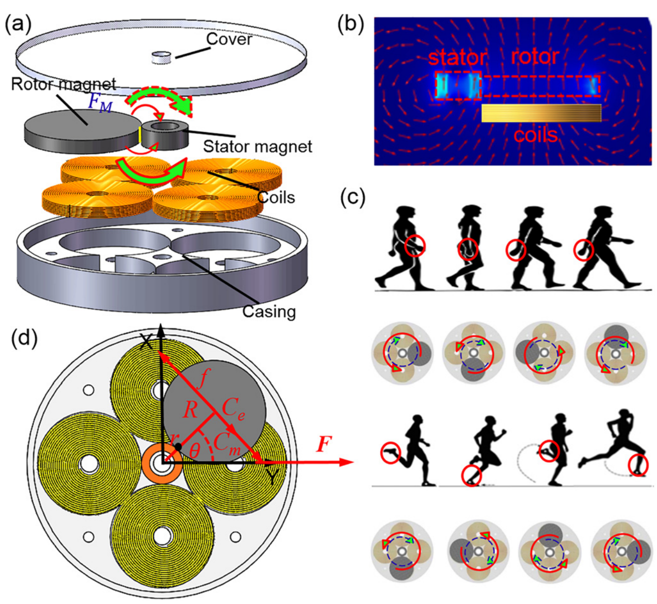

FIG. 1. (a) The physical structure of the REH; (b) the magnetic field distribution of the stator and rotor; (c) two typical application scenarios for the REH, where the rotor magnet of the REH attached on the wrist and ankle does clockwise and anticlockwise rotation around the center stator magnet; and (d) physical model of the REH when the rotor magnet rotates.

$$\begin{cases}(M+m)\ddot{y}+m(R+r)(\ddot{\theta}\cos\theta-\dot{\theta}^2\sin\theta)+c\dot{y} \\ F\cos(\omega t)\left[m(R+r)^2+I\right]\ddot{\theta}+c_m\dot{\theta}+c_e\dot{\theta} \\ =-m(R+r)\ddot{y}\cos\theta.\end{cases} \tag{2}$$

Approximating the magnetic field of the rotor magnet to uniform, the output voltage across each wound coil is only related to the number of turns N, the angular velocity of the rotor, and the radius of the coils. The voltage can be expressed as

$$E(t)=NBLv=NB\int_{point1}^{point2}\dot{\theta}l\,dl\,, \tag{3}$$

where piont1 and point2 are the coordinates of the two points at which the outer diameter of the magnet intersects the coils. When the rotor magnet rotates, there will be electric-magnetic resistance force C_e and rotational damping force C_m. C_e and C_m can be expressed as

$$\begin{cases}C_e=NBIL=B\dfrac{E(t)}{R_C}L=N^2B^2\dfrac{\int_{point1}^{point2}\dot{\theta}l\,dl}{R_c}\displaystyle\int_{point1}^{point2}dl \\ C_m=2mc_m\sqrt{\dfrac{g}{R+r}}(R+r)\dot{\theta},\end{cases} \tag{4}$$

where B means the magnetic field density. Because the stator magnet and rotor magnet attract each other, the magnetic field intensity is relatively lower, and the value in the simulation is small. L is the effective length of the coils when the magnetic induction line cuts the coil; R_c is the impedance of the coils and c_m is the mechanical damping coefficient.

Based on Eqs. (2)–(4), the relationship between the input excitation force F and output voltage $E(t)$ can be investigated by the Matlab/Simulink model. To perform the theoretical simulations, the system parameters are shown in Table I.

In order to investigate the output performance of the REH, the experiment is carried out by using a linear motor to drive the REH as shown in Fig. 2(a). The REH is fixed on the fixed base. The linear motor stage is controlled through a function generator with tunable frequency and amplitude. Figures 2(b) and 2(c) show the theoretical and experimental open circuit voltages of the REH at different frequencies and amplitudes. All the experimental data are acquired by an oscilloscope DSOX2022A without additional load. When the frequency of the excitation force is varied from 0.5 Hz to 5 Hz with the amplitude staying at a constant of 5 cm, the output peak-to-peak voltage increases from 0.1 to 0.9 V, as shown in Fig. 2(b). While the amplitude of the excitation force changes from 1 to 10 cm with the frequency remaining constant of 3 Hz, the output peak-to-peak voltage increases from 0.1 to 1.5 V, as shown in Fig. 2(c). It is verified that in a certain frequency and amplitude range, when the amplitude is constant, the energy harvesting effect increases with the increase in the frequency. However, when the frequency is constant, the larger the amplitude, the better the energy harvesting effect. The experimental results agree well with theoretically derived results, with a small amount of bias between them. Taking a

TABLE I. Identified system parameters.

Parameters	Description	Value
M (kg)	The mass of the housing	1.5
m (kg)	Rotor mass	0.1
R (m)	Rotor radius	0.0125
r (m)	Stator radius	0.005
B (T)	Flux density of the magnets	0.03
c_m	Damping ratio of the rotor	0.02
N	Number of coils	500
R_c (Ω)	Internal resistance	72
c	Damping ratio of the housing	0.3

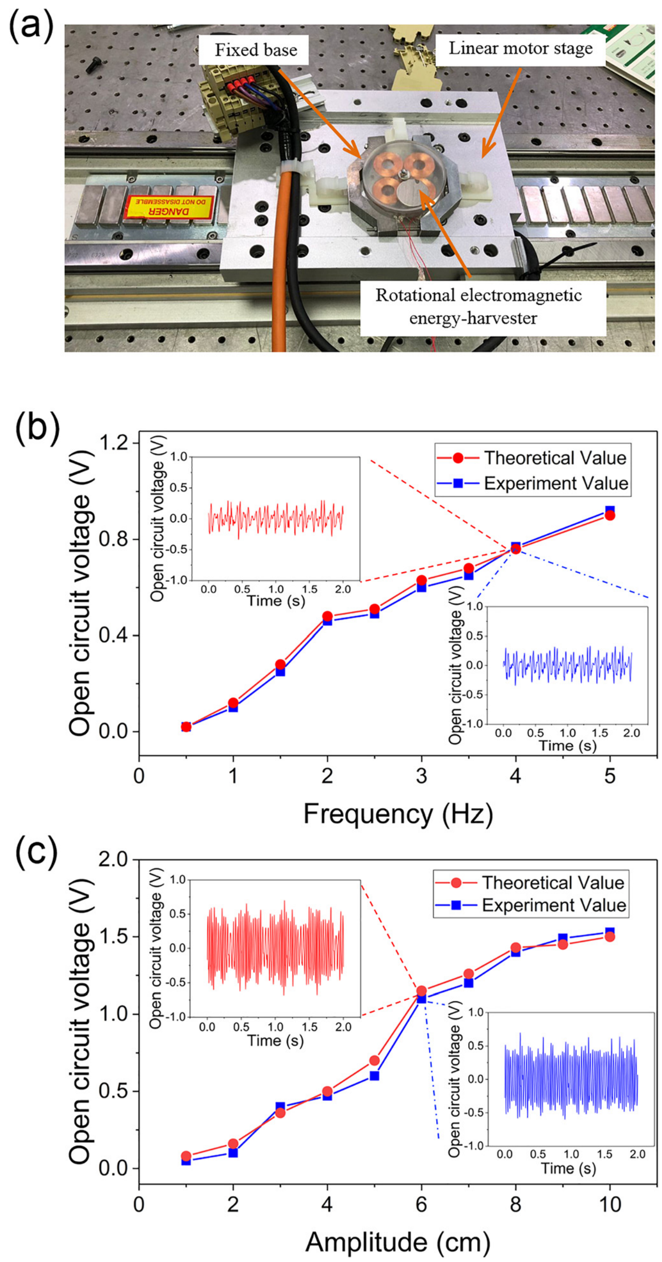

FIG. 2. The output voltage of the fabricated REH tested on the linear motor. (a) The photograph of the REH tested on the linear motor; (b) the output peak-to-peak voltage of the REH for a varied frequency from 0.5 to 5 Hz with a constant amplitude of 5 cm; and (c) the output peak-to-peak voltage of the REH for a varied amplitude from 1 to 10 cm with a constant frequency of 3 Hz.

frequency of 4 Hz and an amplitude of 6 cm of the excitation as instance, the theoretical simulation output voltage is similar to experimental output voltage waveforms with a duration of 2 s as shown in Figs. 2(b) and 2(c).

The experiments are carried out to verify the characteristics of the REH under rotation in horizontal plane, vertical plane, and swing motion conditions. A wireless accelerometer module of MPU-6050 is used to measure the acceleration of the REH. The output waveform of the REH and the acceleration under different motion conditions are shown in Fig. 3. Figure 3(a) shows the REH rotating on the horizontal plane. It can be seen that the z-axis keeps the acceleration of 1 g due to the gravity, and the sinusoidal waveform of the x-axis and y-axis presents an in-plane acceleration of 0.3 g and a frequency of 1.5 Hz. The output peak-to-peak voltage is about 0.69 V. Figure 3(b) shows the REH rotating on the vertical plane at the same frequency. The maximum output peak-to-peak voltage is 0.8 V, which is a little bit larger than that of horizontal rotation. This is because when the REH rotates on the vertical plane, the y-axis direction obtains larger acceleration due to the action of gravity, which makes the rotor's angular velocity faster. In particular, under the action of gravity, the waveform of Fig. 3(b) is less regular than Fig. 3(a). Figure 3(c) shows the wrist swings in four directions (left, right, backward, and forward). The rotor magnet rotates under the action of gravity, the frequency of each action is approximately 0.4 Hz, and the maximum acceleration in the x-axis and y-axis is 0.5 g. The resulting output peak-to-peak voltage is 0.46 V. Compared with Figs. 3(a) and 3(b), distinct crests and troughs can be seen in Fig. 3(c). It is because when the swing motion changes from one phase to the other, the output voltage reaches its maximum immediately and then damped gradually until the next phase change.

It is known that human motion is irregular and complicated. The vibration frequency is extremely low of less than 10 Hz and the motion direction is not always along the

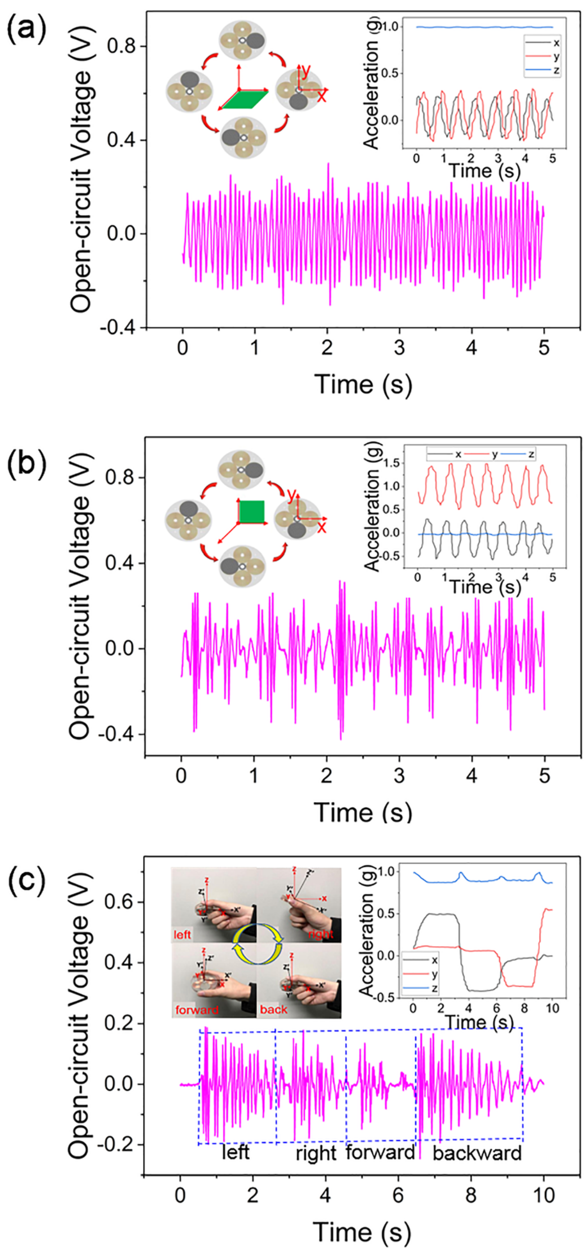

FIG. 3. The acceleration waveform and output peak-to-peak voltage waveform of the REH under different motion conditions: (a) the REH rotates horizontally; (b) the REH rotates vertically; and (c) the REH swings left-right-back-forward.

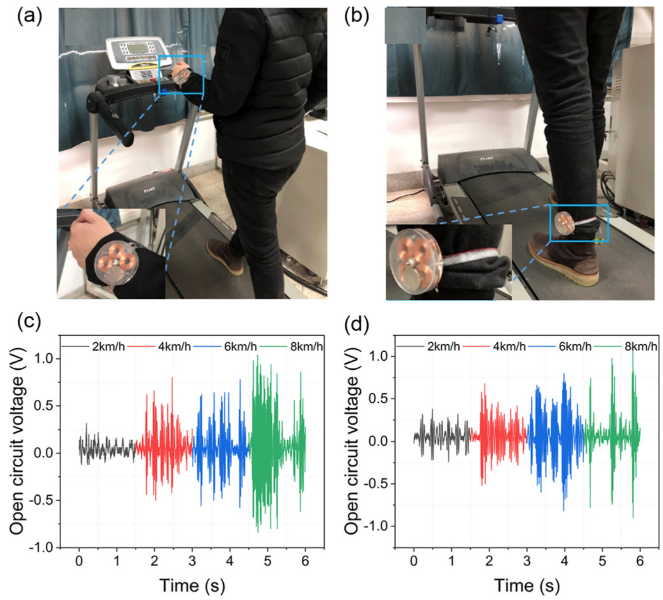

FIG. 4. (a) Photograph of the rotational REH which was attached on the tester's wrist and (b) ankle on a treadmill; (c) open circuit voltage of the rotational REH attached on the tester's wrist and (d) ankle at different running speeds.

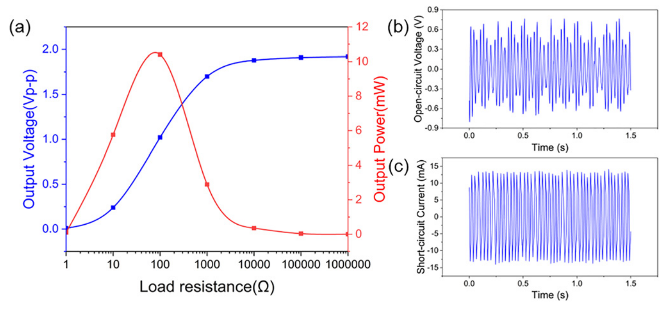

FIG. 5. (a) The output voltage and power under different external loading resistances with a hand shaking frequency of 8 Hz; (b) the open-circuit voltage and (c) short-circuit current of the REH under a rotational frequency of 8 Hz.

TABLE II. Performance comparison among published energy harvesters for human motion.

Author	Mechanism	Volume (cm^3)	Frequency or speed	Power (mW)
Our previous work[9]	Electromagnetic	5.18	6.7 Hz	0.569 mW
Pit *et al.*[16]	Piezoelectric	1.85	25 Hz	0.1 mW
Fan *et al.*[17]	Piezoelectric	32.4	8 km/h	0.35 mW
Halim *et al.*[27]	Electromagnetic	20.1	1 Hz	0.0613 mW
This work	Electromagnetic	33.1	8 Hz	10.4 mW

vertical or horizontal plane. To demonstrate the effectiveness of the energy generation, one participant tester with a weight of 53 kg and a height of 165 cm was walking and running on a treadmill at a speed of 2–8 km/h (2 km/h for walking, 4–6 km/h for jogging, and 8 km/h for running). The REH was attached on the tester's wrist and ankle as illustrated in Figs. 4(a) and 4(b). Figures 4(c) and 4(d) show the voltage waveforms of the REH excited by wrist shaking and ankle moving at different running speeds of 2–8 km/h, respectively. The open-circuit voltages of the REH attached on the wrist reach 0.45, 1.14, 1.35, and 1.81 V at running speeds of 2, 4, 6, and 8 km/h, respectively. The corresponding voltages of the REH attached on the ankle are 0.6, 1.2, 1.5, and 1.92 V, severally. It is obvious that the open-circuit voltages of both the REH attached on the wrist and ankle increase accordingly with increasing speed, where a high-speed running possesses a high vibration amplitude and frequency. Under the action of inertial force, the magnetic rotor is able to rotate rapidly by hand shaking. Figure 5(a) illustrates that the output voltage of the REH increases with the increasing load resistances, resulting in a maximum output power of 10.4 mW under a matched load resistance of 100 Ω. The relative movement between the rotor magnet and wound coils of the REH generates output voltage and current under a hand shaking frequency of 8 Hz as depicted in Figs. 5(b) and 5(c). Some reported devices operated for the human motion energy harvesting are listed in Table II for comparison. It is obvious that the rotational REH provides a relatively good output performance for low-frequency human motion.

In summary, a theoretical model of a non-resonant REH is established based on the rotation characteristic of a rotor. The harvesting performance of the REH is varied with the frequency and amplitude on a linear motor. The detailed output values of the non-resonant REH are experimentally measured, and the corresponding output voltage waveforms show the validity of the theoretical model. As a result, the non-resonant REH is sensitive to harvest energy from human motions with different amplitudes, frequencies, and directions, such as hand shaking, walking, or running. It has the potential capability as a sustainable power source for wearable electronics. Furthermore, the experimental results verify that the non-resonant REH exhibits good performance when it is used to harvest energy from human motion on treadmill.

This work was funded by the National Science Foundation of China (Grant Nos. 41527901 and 61673287), Qingdao National Laboratory for Marine Science and Technology (Grant No. 2017ASKJ01), and HIFES Seed Funding-2017-01 grant (R-263-501-012-133) "Hybrid Integration of Flexible Power Source and Pressure Sensors" at the National University of Singapore.

[1]L. H. Tang and Y. Yang, Appl. Phys. Lett. **101**, 094102 (2012).
[2]K. Fan, Z. Ming, C. Xu, and F. Chao, Chin. Phys. B **22**, 104502 (2013).
[3]S. Li, J. Wang, W. Peng, L. Lin, Y. Zi, S. Wang, G. Zhang, and Z. Wang, Adv. Energy Mater. **7**(13), 1602832 (2017).
[4]B. Meng, X. Cheng, X. Zhang, M. Han, W. Liu, and H. Zhang, Appl. Phys. Lett. **104**, 103904 (2014).
[5]A. Erturk and D. J. Inman, Smart Mater. Struct. **18**, 025009 (2009).
[6]Y. Yang and L. Tang, J. Intell. Mater. Syst. Struct. **20**, 2223–2235 (2009).
[7]M. Kim, M. Hoegen, J. Dugundji, and B. L. Wardle, Smart Mater. Struct. **19**, 045023 (2010).
[8]S. Zhao and A. Erturk, Smart Mater. Struct. **22**, 015002 (2013).
[9]H. Liu, S. Gudla, F. A. Hassani, C. Heng, Y. Lian, and C. Lee, IEEE Sens. J. **15**(4), 2356 (2015).
[10]H. Liu, Z. Ji, T. Chen, L. Sun, S. C. Menon, and C. Lee, IEEE Sens. J. **15**(9), 4782 (2015).
[11]B. Yang, C. Lee, W. Xiang, J. Xie, J. He, R. K. Kotlanka, S. P. Low, and H. Feng, J. Micromech. Microeng. **19**(3), 035001 (2009).
[12]H. Liu, B. W. Soon, N. Wang, C. J. Tay, C. G. Quan, and C. Lee, J. Micromech. Microeng. **22**(12), 125020 (2012).
[13]H. Liu, K. H. Koh, and C. Lee, Appl. Phys. Lett. **104**(5), 053901 (2014).
[14]R. K. Gupta, Q. Shi, L. Dhakar, T. Wang, C. Heng, and C. Lee, Sci. Rep. **7**, 41396 (2017).
[15]H. Liu, Y. Qian, N. Wang, and C. Lee, J. Microelectromech. Syst. **23**(3), 740–749 (2014).
[16]P. Pillatsch, E. M. Yeatman, A. S. Holmes, and P. K. Wright, Sens. Actuator, A **244**, 77 (2016).
[17]K. Fan, Z. Liu, H. Liu, L. Wang, Y. Zhu, and B. Yu, Appl. Phys. Lett. **110**(14), 143902 (2017).
[18]J. Cao, W. Wang, S. Zhou, D. J. Inman, and J. Lin, Appl. Phys. Lett. **107**(14), 143904 (2015).
[19]J. Cao, S. Zhou, W. Wang, and J. Lin, Appl. Phys. Lett. **106**(17), 173903 (2015).
[20]S. Zhou, J. Cao, D. J. Inman, S. Liu, W. Wang, and J. Lin, Appl. Phys. Lett. **106**(9), 093901 (2015).
[21]W. Wang, J. Cao, C. R. Bowen, D. J. Inman, and J. Lin, Appl. Phys. Lett. **112**(21), 213903 (2018).
[22]D. Spreemann, B. Folkmer, D. Mintenbeck, and Y. Manoli, in *Proceedings of Power MEMS* (2005), pp. 144–146.
[23]C. T. Pan and T. Wu, J. Micromech. Microeng. **17**(1), 120 (2007).
[24]B. Yang, C. Lee, R. K. Kotlanka, J. Xie, and S. P. Lim, J. Micromech. Microeng. **20**(6), 065017 (2010).
[25]C. Lu, Y. Wang, C. Sung, and Paul C. Chao, IEEE Trans. Magn. **47**(10), 2395 (2011).
[26]C. Lu, C. Wang, C. Sung, and Paul C. Chao, J. Vib. Acoust. **133**(1), 014501 (2011).
[27]M. A. Halim, R. Rantz, Q. Zhang, L. Gu, K. Yang, and S. Roundy, Appl. Energy **217**, 66 (2018).